Channel Estimation and Compensation for Preamble-Assisted DAPSK Transmission in Digital Mobile Radio System

Der-Zheng Liu, *Student Member, IEEE,* and Che-Ho Wei, *Fellow, IEEE*

***Abstract*—This paper presents a novel channel estimation and compensation technique, combining fading estimation and frequency offset estimation, for preamble-assisted differentially encoded amplitude- and phase-shift keying (DAPSK) transmission in the digital mobile radio system. The received preamble symbols are used to estimate the combined distortions caused by multipath fading and frequency offset. The detected data symbols as well as preamble symbols are used to enhance the accuracy of the estimation process. The combined distortions can be compensated in the data symbols at the same time. The storage-delay time of the estimation process is only several symbols long. A series of computer simulations have been carried out to investigate the bit error rate performances of the preamble-assisted 16-DAPSK signals with uncertain frequency offset in the frequency-nonselective and frequency-selective Rayleigh fading channels.**

***Index Terms*—Channel compensation, channel estimation, differentially encoded amplitude- and phase-shift keying (DAPSK), fading channel, frequency offset, preamble.**

I. Introduction

RECENTLY, there has been growing interest in applying multilevel modulations, such as quadrature amplitude modulation (QAM), differentially encoded phase-shift keying (DPSK), and differentially encoded amplitude- and phase-shift keying (DAPSK), with higher spectral efficiency to the burst-mode high-data-rate digital mobile radio systems [1]–[4]. In mobile environments, the amplitude and phase of received signals are perturbed randomly by both additive white Gaussian noise (AWGN) and multipath fading [5]. Multipath fading, which introduces severely time-varying amplitude and phase distortion to signal waveforms, obstructs the receiver to recover reliable amplitude and phase references for data detection. The irreducible bit error rate (BER) caused by multipath fading inhibits the use of multilevel modulations. However, channel compensation techniques and differential detection techniques have been studied to mitigate multipath fading in the multilevel modulation transmission, respectively [4].

Manuscript received February 1, 1999; revised July 25, 2000. This work was supported by the MTI Center for Networking Research, National Chiao Tung University, Hsinchu, Taiwan, R.O.C., and by the National Science Council of the Republic of China under Grant NSC87-2218-E-009-054. This paper was presented in part at the 10th International Symposium on Personal, Indoor and Mobile Radio Communications (PIMRC'99), Osaka, Japan, September 12–15, 1999.

The authors are with the Department of Electronics Engineering, National Chiao Tung University, Hsinchu, Taiwan, R.O.C. (e-mail: dzliu.ee84g@nctu.edu.tw; chwei@cc.nctu.edu.tw).

Publisher Item Identifier S 0018-9545(01)03074-2.

Two types of conventional channel sounding schemes, pilot tone-aided scheme and pilot symbol-aided scheme, can be used to suppress the irreducible BER and enable the multilevel modulations with coherent detection. In a pilot tone-aided scheme, such as transparent tone-in-band (TTIB) [6], [7], the pilot tone provides the receiver with an explicit amplitude and phase reference for data detection. This scheme requires relatively complex signal processing and results in an increased peak-to-average power ratio. In the pilot symbol-aided scheme, the channel distortion can be estimated by the received pilot symbol [8]–[10] and then used to correct the fading effects in the data symbols.

However, in the pilot symbol-aided scheme, the storage-delay time for the process is at least one frame long even by using a simple first-order estimation technique [10], as illustrated in Fig. 2. Furthermore, most previous works on pilot symbol-aided modulation system assumed that the frequency offset produced negligible degradation. If a less accurate oscillator is employed and nontrivial frequency offset is not properly compensated, a significant loss in performance or in throughput rate would result [11]. Consequently, frequency offset estimation is required to relieve the stringent requirements on the oscillator's accuracy and stability. A frequency offset compensation of pilot symbol-assisted modulation (PSAM) transmission using maximum-likelihood estimators (MLEs) has been investigated by Kuo and Fitz [12] in the frequency-nonselective fading channel. The frequency offset can be estimated from the demodulated pilot symbols. However, the acquisition time is needed at least several frames long.

In this paper, we consider the DAPSK modulation, which was first proposed in [13] and further studied for application in high-data-rate wireless communications [14]–[19]. The major advantage of DAPSK modulation is its robustness to fast channel variation and simplicity in demodulation, because it allows a simple differential detection without tracking the absolute amplitude and phase of received signals. Several studies in the differential detection of DAPSK have been presented in [20]–[23]. A noncoherent detection scheme for the preamble-assisted DAPSK transmission was presented and analyzed in [23]. This scheme yields an error performance approaching that of the QAM scheme with ideal coherent detection within a loss of approximately 1 dB in AWGN channel.

Here, we focus on the channel estimation and compensation techniques of a preamble-assisted DAPSK transmission for coherent differential detection. The frame structure of the preamble-assisted DAPSK transmission system is illustrated in Fig. 1. The receiver is assumed to have *a priori* knowledge of

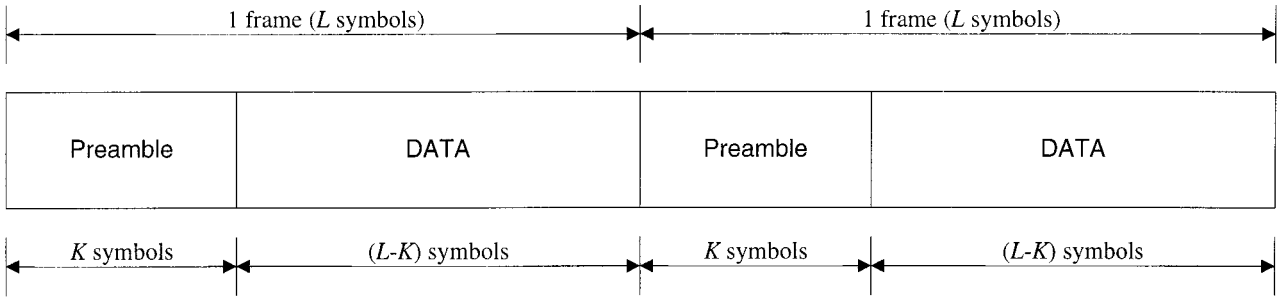

Fig. 1. Frame structure of preamble-assisted DAPSK transmission system.

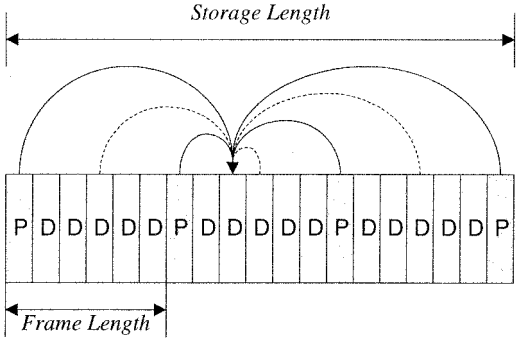

Fig. 2. Storage-delay time of pilot symbol-aided scheme ($K = 1$ and $L = 6$).

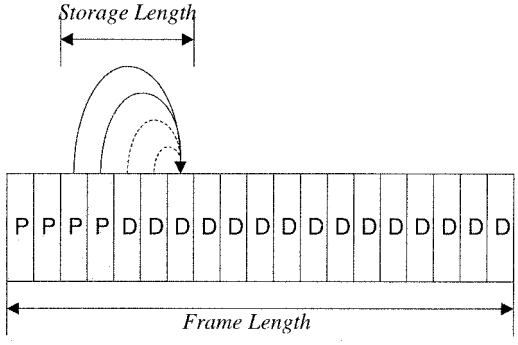

Fig. 3. Storage-delay time of preamble-assisted scheme ($K = 4$ and $L = 19$).

the preamble sequence, and so is able to extract the preamble symbols from the received signal. The received preamble symbols are used to estimate the combined distortions caused by multipath fading and frequency offset. In the proposed scheme, detected data symbols as well as preamble symbols are used to enhance the accuracy of estimation process. The storage-delay time for the process can be reduced to only several symbols long, as illustrated in Fig. 3. At the same time, signal distortions caused by multipath fading and frequency offset can be compensated in the data symbols. The major difference between our proposed scheme and Chung's scheme in [23] is that preamble symbols are used in the proposed channel estimation to achieve the coherent differential detection, rather than the noncoherent differential detection of DAPSK signals.

This paper is organized as follows. Section II describes the preamble-assisted DAPSK transceiver and the channel model used in the simulations. The proposed preamble-assisted channel estimation and compensation technique is described in Section III. The BER performance of the proposed preamble-assisted scheme is presented in Section IV and compared with the pilot symbol-aided scheme for coherent detection and the differential detection scheme for noncoherent detection. A brief conclusion is given in Section V.

II. Preamble-Assisted DAPSK System and Channel Model

The preamble-assisted DAPSK transceiver and the equivalent-baseband channel model are shown in Fig. 4.

A. Transmitter

In the transmitter, the preamble symbols are packaged and inserted into a frame in front of data symbols for transmission. The transmitter sequentially encodes information bits onto the amplitude ratio and phase difference between two consecutive transmitted symbols. In the preamble-assisted modulation transmission, each frame consists of one preamble block of K symbols followed by one data block of $(L-K)$ symbols, as shown in Fig. 1. Note that the preamble-assisted modulation transmission with $K = 1$ corresponds to the PSAM transmission.

The M-ary DAPSK (MDAPSK) modulation with N_a concentric amplitude rings, each containing N_p phases, where $N_a \cdot N_p = M$, can be further described as follows. A sequence of $m = \log_2 M$ transmitted bits is first grouped and mapped by Gray labeling into one of M independent symbol pairs $(\Delta a_k^{(i)}, \Delta b_k^{(i)})$ according to MDAPSK signal constellation, where

$$\Delta a_k^{(i)} \in \{0, 1, \ldots, N_a - 1\} \tag{1}$$

$$\Delta b_k^{(i)} \in \{0, 1, \ldots, N_p - 1\}. \tag{2}$$

For $k = 0, 1, \ldots, L-1$, the kth MDAPSK symbols of the ith frame is given in the complex form by

$$s_k^{(i)} = \lambda \mu^{a_k^{(i)}} e^{j(2\pi/N_p) b_k^{(i)}} \tag{3}$$

where $\mu > 1$ is a fixed ring-ratio and

$$\lambda = \sqrt{N_a(\mu^2 - 1)/(\mu^{2N_a} - 1)} \tag{4}$$

is the normalized-gain of the MDAPSK symbols, that is, the average transmitted signal power is normalized to unity. $a_k^{(i)}$ and

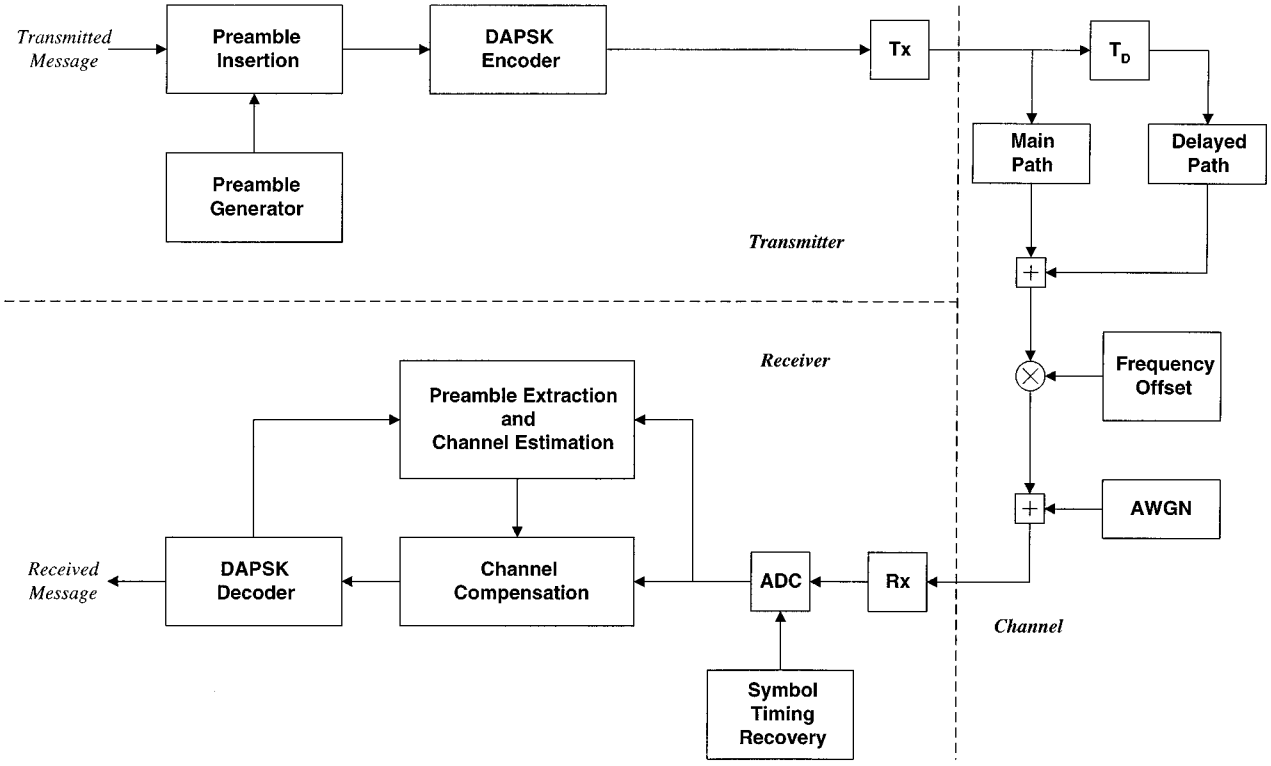

Fig. 4. Preamble-assisted DAPSK transmission system and channel model.

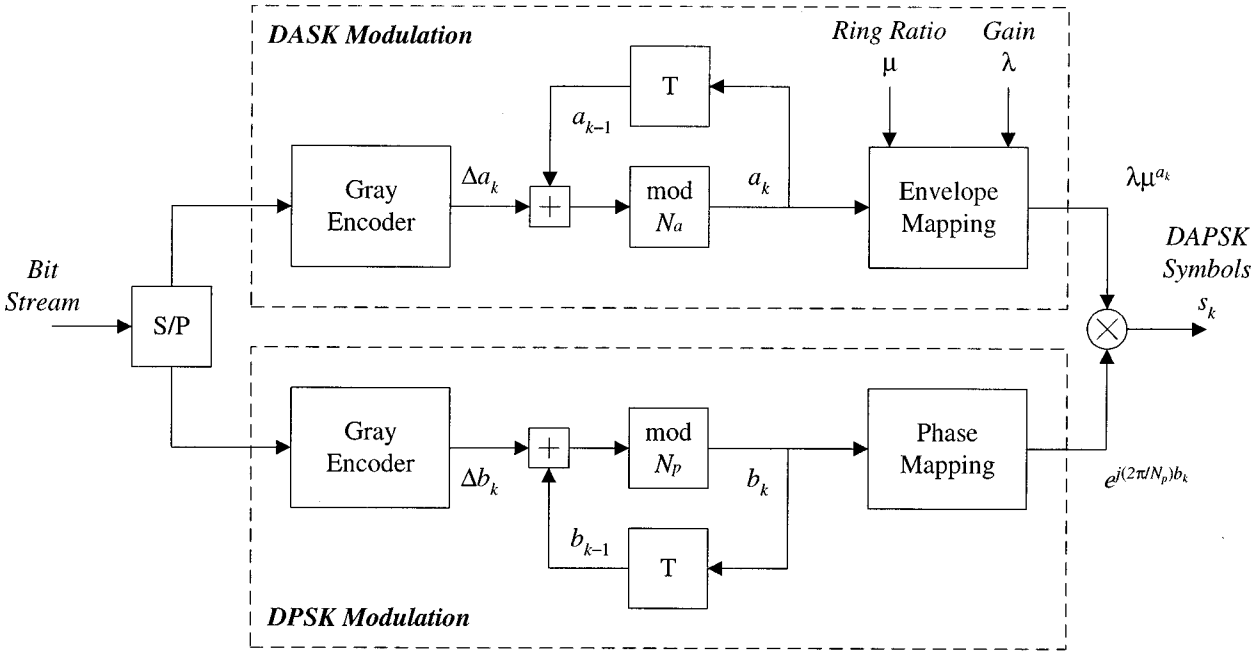

Fig. 5. A DAPSK encoder.

$b_k^{(i)}$ indicate the amplitude and phase levels of the transmitted symbols $s_k^{(i)}$ and are related to $\Delta a_k^{(i)}$ and $\Delta b_k^{(i)}$ by

$$a_k^{(i)} = \left(a_{k-1}^{(i)} + \Delta a_k^{(i)}\right) \bmod N_a \quad (5)$$

$$b_k^{(i)} = \left(b_{k-1}^{(i)} + \Delta b_k^{(i)}\right) \bmod N_p \quad (6)$$

respectively. Therefore, an MDAPSK encoder can be treated as a combination of an N_a-ary differentially encoded amplitude-shift keying (N_aDASK) encoder and an N_p-ary differentially encoded phase-shift keying (N_pDPSK) encoder, as illustrated in Fig. 5. Note that MDAPSK modulation with $N_a = 1$ corresponds to MDPSK modulation.

B. Channel Model

Here, we consider that the multipath fading channel is frequency nonselective and modeled as a Rayleigh fading channel. The Rayleigh fading process was generated according to Jakes' model [5], where the correlation function of fading process is given as

$$R(\tau) = J_0(2\pi f_D \tau) \tag{7}$$

where f_D is the maximum Doppler shift of the fading signal caused by the mobile motion. The Doppler shift is given by $f_D = v/\lambda$, where v is the velocity of the mobile and λ is the wavelength of the carrier. In general, the normalized maximum Doppler shift $f_D T$ is used as the measure for the fading rate, where T denotes the symbol duration.

The equivalent-baseband signal at the receiver is given by

$$r(t) = \sqrt{\frac{\Gamma_S}{2}} \cdot e^{j(\Delta\omega t+\theta)} \cdot f(t) \cdot \sum_{i=-\infty}^{\infty} \sum_{k=0}^{L-1} s_k^{(i)} \cdot g_T[t-(iL+k)T] + w(t) \tag{8}$$

where $g_T(t)$ is the pulse-shaping filter and Γ_S denotes the average received signal-to-noise ratio (SNR) per symbol. Thus the average SNR per bit is given by

$$\Gamma_b = \Gamma_S / \log_2 M. \tag{9}$$

$w(t)$ is a complex Gaussian process whose real and imaginary components have the same power spectral density (PSD) with $N_0 = 1$. $f(t)$ represents the combined distortion introduced into the desired signal in the fading channel. $\Delta\omega = 2\pi\Delta f$ and θ are frequency offset in radian and residual phase error introduced during demodulation, respectively.

C. Receiver

We assume that the pulse-shaping filter $g_T(t)$ in the transmitter has a square-root raised-cosine (SRRC) shape with a rolloff factor α; and that the matched filter $g_R(t) = g_T(-t)/T$ at the receiver has similar SRRC shape. The demodulated signal $y(t)$ after the matched filter is given by

$$y(t) = r(t) \otimes g_R(t) \tag{10}$$

where the symbol $\otimes$ denotes the time convolution process.

Assuming that the maximum Doppler shift f_D due to mobile motion is far smaller than the symbol rate $1/T$, i.e., the fading rate is small, then the intersymbol interference (ISI) caused by the filtering process can be neglected. Therefore, the demodulated signal after the matched filter can be simplified as

$$y(t) \approx \sqrt{\frac{\Gamma_S}{2}} \cdot e^{j(\Delta\omega t+\theta)} \cdot f(t) \cdot \sum_{i=-\infty}^{\infty} \sum_{k=0}^{L-1} s_k^{(i)} \cdot g[t-(iL+k)T] + n(t) \tag{11}$$

where $g(t) = g_T(t) \otimes g_R(t)$ is a raised-cosine Nyquist pulse with $g(0) = 1$ and $n(t) = w(t) \otimes g_R(t)$ is a filtered Gaussian process.

The demodulated signal after the matched filter is sampled and digitized through the analog-to-digital converter (ADC) driven by the sampling instants $t_k^{(i)}$ provided by symbol timing recovery. We have that

$$t_k^{(i)} = (iL+k)T + \tau_k^{(i)} \tag{12}$$

where $\tau_k^{(i)}$ denotes the sampling timing error. The on-time samples of the ith frame

$$y_k(i) = y(t)\big|_{t=t_k^{(i)}} \tag{13}$$

are used for the detector and decoder.

Assuming that the baseband received signal is sampled in synchronism, i.e., $\tau_k(i) = 0$, the sampled signal at time $t = (iL+k)T$ is given by

$$y_k^{(i)} \approx \sqrt{\frac{\Gamma_S}{2}} \cdot e^{j(k\Delta\omega T+\theta)} \cdot f_k^{(i)} \cdot s_k^{(i)} + n_k^{(i)} \tag{14}$$

where

$n_k^{(i)} = n(t)\big\|_{t=(iL+k)T}$	noise term;
$f_k^{(i)} = f(t)\big\|_{t=(iL+k)T}$	combined distortion due to multipath fading;
$\Delta\omega T$ and θ	normalized frequency offset in radian and residual phase error, respectively.

To reduce the performance degradation by channel distortions caused by multipath fading and frequency offset, channel estimation and compensation described in Section III are adopted in front of the DAPSK decoder.

D. DAPSK Demodulation

The DAPSK decoder is a combination of an amplitude-level decoder and a phase-level decoder, as illustrated in Fig. 6. The amplitude and phase level of the compensated symbols $z_k^{(i)}$ obtained through the envelope-level detector and phase-level detector are given by

$$\tilde{a}_k^{(i)} = \log_\mu \left(\left| z_k^{(i)} \right| \right) \tag{15}$$

$$\tilde{b}_k^{(i)} = \frac{N_p}{2\pi} \cdot \mathrm{Arg}\left(z_k^{(i)} \right) \tag{16}$$

respectively. The change of amplitude and phase levels between two consecutive compensated symbols can be computed as

$$\Delta\tilde{a}_k^{(i)} = \tilde{a}_k^{(i)} - \tilde{a}_{k-1}^{(i)} \tag{17}$$

$$\Delta\tilde{b}_k^{(i)} = \tilde{b}_k^{(i)} - \tilde{b}_{k-1}^{(i)} \tag{18}$$

respectively. The differentially detected symbol pairs $(\Delta\tilde{a}_k^{(i)}, \Delta\tilde{b}_k^{(i)})$ of MDAPSK signals are obtained by comparing with the decision thresholds and then taking modulo-operations as

$$\Delta\hat{a}_k^{(i)} = \left\lfloor \tilde{a}_k^{(i)} \right\rfloor \bmod N_a \tag{19}$$

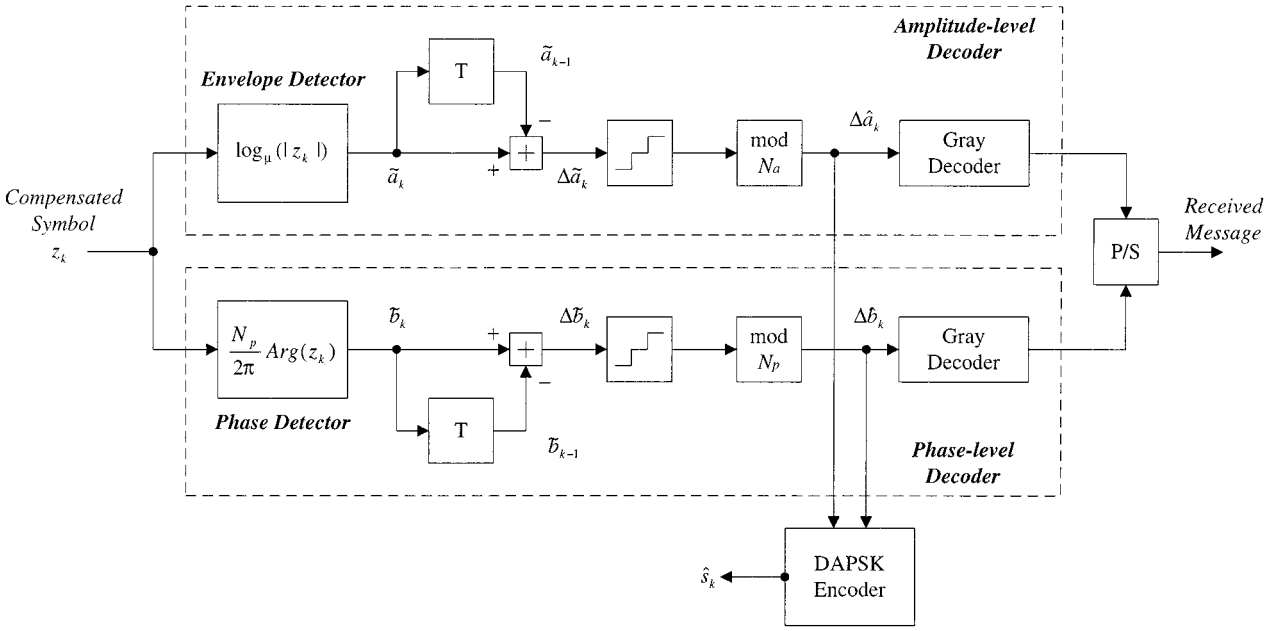

Fig. 6. A DAPSK decoder combined with an amplitude-level decoder and a phase-level decoder.

$$\Delta\hat{b}_k^{(i)} = \left\lfloor \tilde{b}_k^{(i)} \right\rfloor \bmod N_p \tag{20}$$

respectively, where $\lfloor\cdot\rfloor$ denotes the roundoff operation. The received bit sequence is mapped by Gray labeling from the differentially detected symbol pairs $(\Delta\hat{a}_k^{(i)}, \Delta\hat{b}_k^{(i)})$ according to the MDAPSK signal constellation, where

$$\Delta\hat{a}_k^{(i)} \in \{0, 1, \ldots, N_a - 1\} \tag{21}$$
$$\Delta\hat{b}_k^{(i)} \in \{0, 1, \ldots, N_p - 1\}. \tag{22}$$

The kth detected MDAPSK symbol of the ith frame in complex form is given by

$$\hat{s}_k = \lambda\mu^{\hat{a}_k^{(i)}} e^{j(2\pi/N_p)\hat{b}_k^{(i)}} \tag{23}$$

where the ring ratio μ and normalized gain λ are the same as that in the DAPSK encoder

$$\hat{a}_k = (\hat{a}_{k-1} + \Delta\hat{a}_k) \bmod N_a \tag{24}$$
$$\hat{b}_k = (\hat{b}_{k-1} + \Delta\hat{b}_k) \bmod N_p \tag{25}$$

indicate the amplitude and phase levels of the detected MDAPSK symbol $\hat{s}_k^{(i)}$, which are related to the differentially detected symbol pairs $(\Delta\tilde{a}_k^{(i)}, \Delta\tilde{b}_k^{(i)})$, respectively.

In the absence of AWGN and with the optimal channel compensation, the compensated symbols are very close to the transmitted symbols, i.e., $z_k^{(i)} \approx s_k^{(i)}$. Therefore, the amplitude and phase levels of the compensated MDAPSK symbols are given by

$$\tilde{a}_k^{(i)} \approx \log_\mu(\lambda) + a_k^{(i)} \tag{26}$$

$$\tilde{b}_k^{(i)} \approx b_k^{(i)} \tag{27}$$

and then the amplitude and phase levels of the detected MDAPSK symbols are obtained as

$$\Delta\hat{a}_k^{(i)} = \Delta a_k^{(i)} \tag{28}$$
$$\Delta\hat{b}_k^{(i)} = \Delta b_k^{(i)} \tag{29}$$

respectively.

III. Channel Estimation and Compensation

Since the preamble symbols are known at the receiver, in the absence of AWGN, the channel distortions in the preamble block, for $k = 0, 1, \ldots, K-1$, can be obtained by

$$\overline{f}_k^{(i)} = \frac{y_k^{(i)}}{p_k^{(i)}} = \sqrt{\frac{\Gamma_S}{2}} \cdot e^{j(k\Delta\omega T + \Delta\theta)} \cdot f_k^{(i)} \tag{30}$$

where $p_k^{(i)} = s_k^{(i)}$ is the kth preamble symbol of the ith frame. The estimate of normalized frequency offset (in radian) $\Delta\omega T$ due to the Doppler shift and the mismatch of local oscillator (LO) in the receiver can be obtained by

$$\Delta\overline{\omega}\,T = \text{Arg}\left\{\frac{\overline{f}_k^{(i)}}{\overline{f}_{k-1}^{(i)}}\right\} = \text{Arg}\left\{\frac{f_k^{(i)}}{f_{k-1}^{(i)}} \cdot e^{\Delta\omega T}\right\}. \tag{31}$$

However, in the presence of AWGN, the estimates of channel distortions in the preamble block, for $k = 0, 1, \ldots, K-1$, are calculated as

$$\hat{f}_k^{(i)} = \frac{y_k^{(i)}}{p_k^{(i)}}. \tag{32}$$

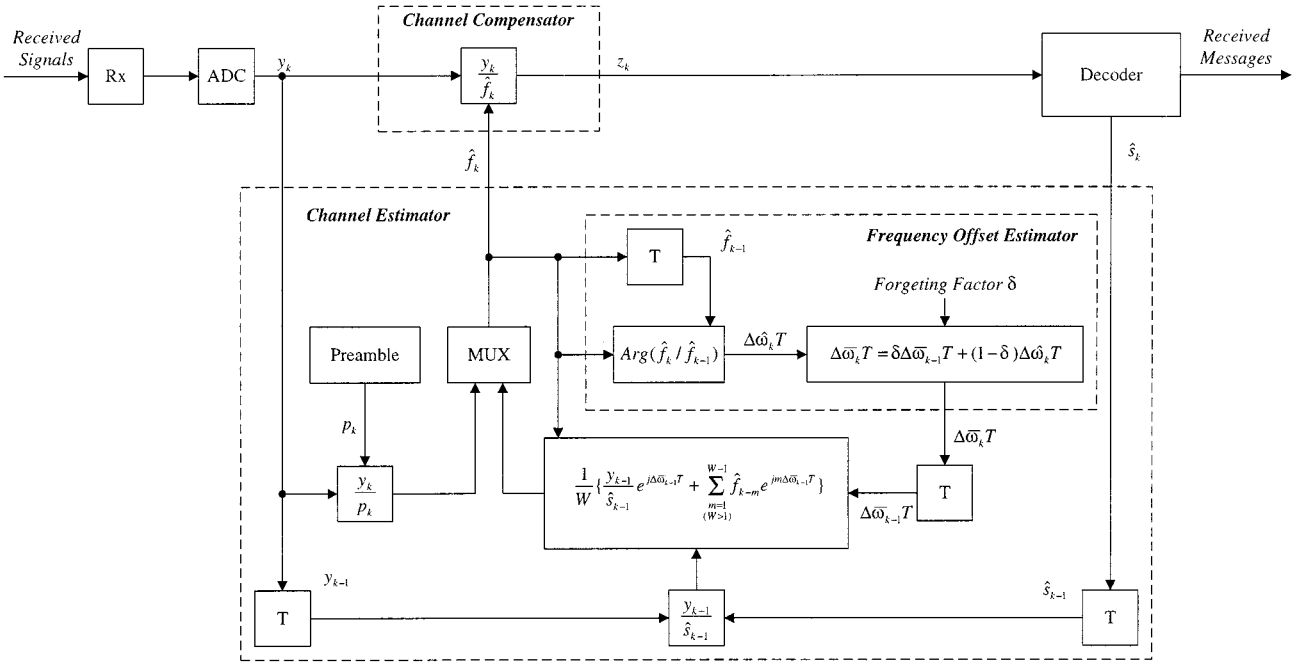

Fig. 7. Proposed channel estimation and compensation scheme.

The instantaneous estimate of normalized frequency offset in radian at the kth symbol of the ith frame is calculated as

$$\Delta\hat{\omega}T = \text{Arg}\left\{\frac{\hat{f}_k^{(i)}}{\hat{f}_{k-1}^{(i)}}\right\}. \tag{33}$$

In the proposed channel estimation, the detected data symbols as well as the preamble symbols are used to enhance the accuracy of estimation process. In the data block, the previous estimates of channel distortions and normalized frequency offset are used to estimate the current channel distortion and normalized frequency offset. There exists a phase rotation $m\Delta\omega T$ between $\hat{f}_k^{(i)}$ and $\hat{f}_{k-m}^{(i)}$, caused by frequency offset. Therefore, the estimates of channel distortions on the data symbols, for $k = K, K+1, \ldots, L-1$, are calculated as

$$\hat{f}_k^{(i)} = \frac{1}{W}\left\{\frac{y_{k-1}^{(i)}}{\hat{s}_{k-1}^{(i)}} \cdot e^{j\Delta\overline{\omega}_{k-1}^{(i)}T} + \sum_{m=1,\,(W>1)}^{W-1} \hat{f}_{k-m}^{(i)} \cdot e^{jm\Delta\overline{\omega}_{k-1}^{(i)}T}\right\} \tag{34}$$

where W is the window size of a moving average filter. The choice of a suitable window size of the moving average filter is a tradeoff between the accuracy of estimation process and the complexity in implementation. The estimate of normalized frequency offset is updated recursively through an exponentially weighted (EW) filter, for $k = 1, 2, \ldots, L-1$, and given by

$$\Delta\overline{\omega}_k^{(i)}T = \delta \cdot \Delta\overline{\omega}_{k-1}^{(i)}T + (1-\delta) \cdot \Delta\hat{\omega}_k^{(i)}T \tag{35}$$

where δ is the forgetting factor, $0 < \delta < 1$. The choice of the forgetting factor of the EW filter is a tradeoff between convergence speed and mean square error (MSE) in steady state. The estimates of channel distortions are used to correct the data symbols, and the compensated symbols, for $k = 0, 1, \ldots, L-1$, are obtained as

$$z_k^{(i)} = \frac{y_k^{(i)}}{\hat{f}_k^{(i)}}. \tag{36}$$

The compensated symbols are then fed into the detector and decoder to produce the detected symbol $\hat{s}_k^{(i)}$ and the binary data at the output. The proposed channel estimation and compensation scheme is illustrated in Fig. 7.

IV. Computer Simulations

A series of computer simulations have been carried out to investigate the BER performances of the preamble-assisted 16-DAPSK signals not only in the frequency-nonselective but also in the frequency-selective fading channels.

The frequency-selective fading channel is modeled as a two-ray Rayleigh fading channel [24] with the time delay T_D between the main path and the delayed path. Each of the transmission paths introduces uncorrelated Rayleigh fading distortion to the corresponding transmitted signal. The main-path-to-delayed-path power ratio is defined as SDR $= 10\log(S/D)$, where S and D are the signal power of the main path and delayed path, respectively. When SDR $= 0$ dB, the signal powers of the main path and delayed path are equal. The normalized delay between the signals from the main path and delayed path is defined as T_D/T. However, this channel model becomes frequency nonselective when SDR $= \infty$ dB or $T_D = 0.0$.

Moreover, the signal-to-noise ratio is defined as SNR $= 10\log(E_S/N_0)$. The normalized frequency offset is defined as $\Delta fT = \Delta\omega T/2\pi$, and $\Delta fT = 0.0$ in the absence

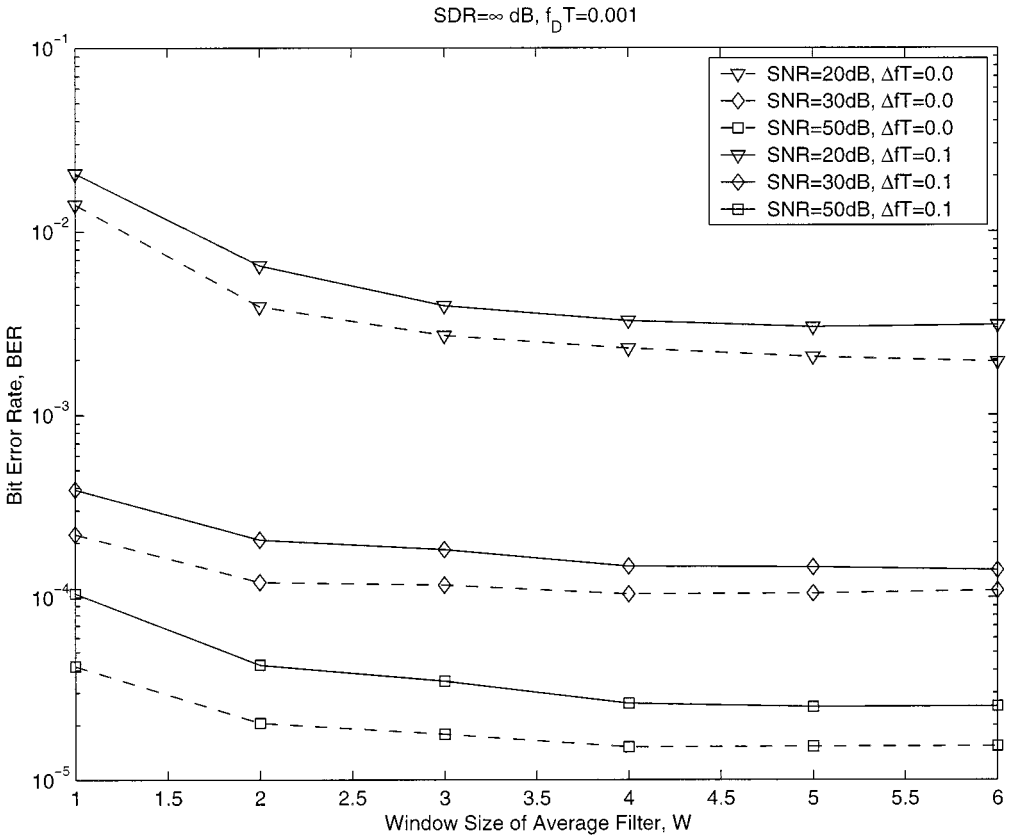

Fig. 8. BER performance versus window size W of moving average filter in frequency-nonselective fading environments (SDR $= \infty$ dB and $f_D T = 0.001$).

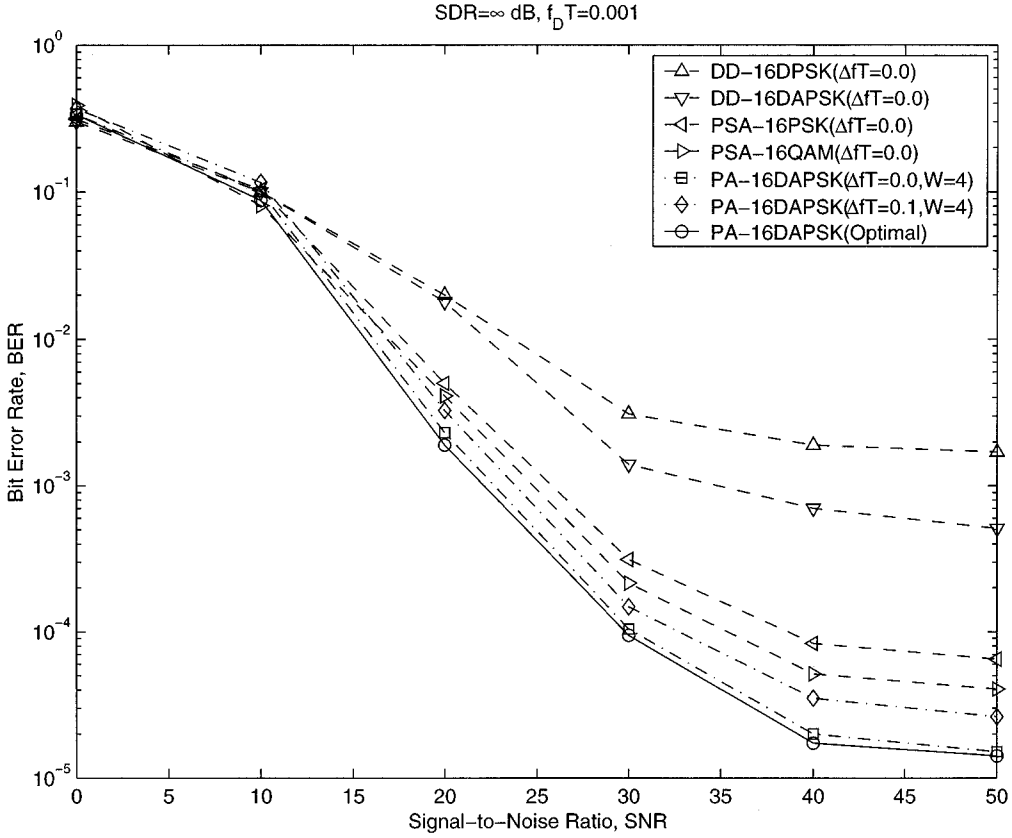

Fig. 9. BER performance versus SNR in frequency-nonselective fading environments (SDR $= \infty$ dB and $f_D T = 0.001$).

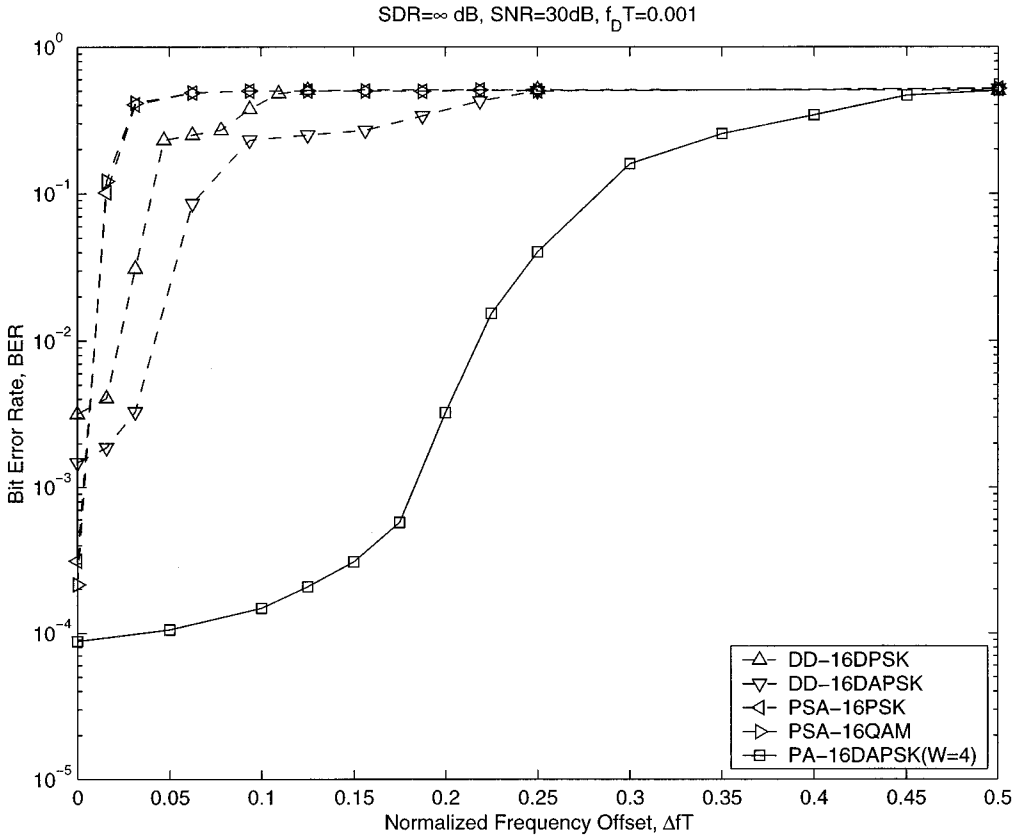

Fig. 10. BER performance versus normalized frequency offset ΔfT in frequency-nonselective fading environments (SDR $= \infty$ dB, SNR $= 30$ dB, and $f_D = 0.001$).

of frequency offset. The normalized maximum Doppler shift, or the fading rate, is defined as f_DT, and $f_DT = 0.0$ in the absence of the fading distortion.

Furthermore, the parameters of the simulation system are described as follows. In the proposed preamble-assisted scheme and the noncoherent differential detection scheme, the frame length $L = 100$ and the preamble length $K = 4$. In the pilot symbol-aided scheme, $L = 25$, and $K = 1$. A symbol rate of $1/T = 100$k symbols per second are used throughout the simulations. The signal constellation of 16-DAPSK modulation contains two concentric amplitude rings, each containing eight phases, i.e., $N_a = 2$, $N_p = 8$. The ring ratio μ of 16-DAPSK signals equals to 2.0. Therefore, the normalized gain λ is $\sqrt{0.4}$. The rolloff factor α of the SRRC filter equals 0.5. The forgetting factor δ of the EW filter in frequency offset estimation is 0.5.

A. Frequency-Nonselective Fading Channels

Fig. 8 shows that the BER performance versus the window size W of the moving average filter in frequency-nonselective fading environments (SDR $= \infty$ dB and $f_DT = 0.001$). The dashed lines show the BER performance in the absence of frequency offset ($\Delta fT = 0.0$). The solid lines show the BER performance with a frequency offset ($\Delta fT = 0.1$). From the simulation results, the suitable window size of the moving average filter is chosen as $W = 4$ for the accuracy of estimation process and the complexity in implementation.

The BER performance versus the SNR per symbol in frequency-nonselective fading environments (SDR $= \infty$ dB and $f_DT = 0.001$) is shown in Fig. 9. The dashed lines show the BER performances of the schemes referred to in [10], where "DD-16DPSK" and "DD-16DAPSK" denote the BER performances of 16-DPSK and 16-DAPSK signals with noncoherent differential detection and "PSA-16PSK" and "PSA-16QAM" denote the BER performances of 16-PSK and 16-QAM signals with the pilot symbol-aided technique for fading compensation, respectively. The lines marked with "PA-16DAPSK" show the BER performances of 16-DAPSK signals with the proposed preamble-assisted channel compensation, where "Optimal" denotes that the receiver has the knowledge of frequency offset and fading effect, so there is no estimation error. We can see that the proposed preamble-assisted scheme outperforms the other schemes even with a frequency offset ($\Delta fT = 0.1$).

Fig. 10 shows that the BER performance versus the normalized frequency offset ΔfT in frequency-nonselective fading environments (SDR $= \infty$ dB, SNR $= 30$ dB, and $f_DT = 0.001$). From the simulation results, we can see the improvement in the suppression of frequency offset for the proposed preamble-assisted channel compensation. Since frequency offset contributes a continuous phase rotation in signal waveforms, the BER performances of PSA-16PSK and PSA-16QAM signals are degraded severely with the increase of frequency offset ($\Delta fT > 0$). However, frequency offset contributes a constant phase rotation ($2\pi\Delta fT$) for DPSK and DAPSK signals after differential detection, the BER performance of noncoherent differential detection is degraded rapidly when the normalized frequency offset is close to the boundary,

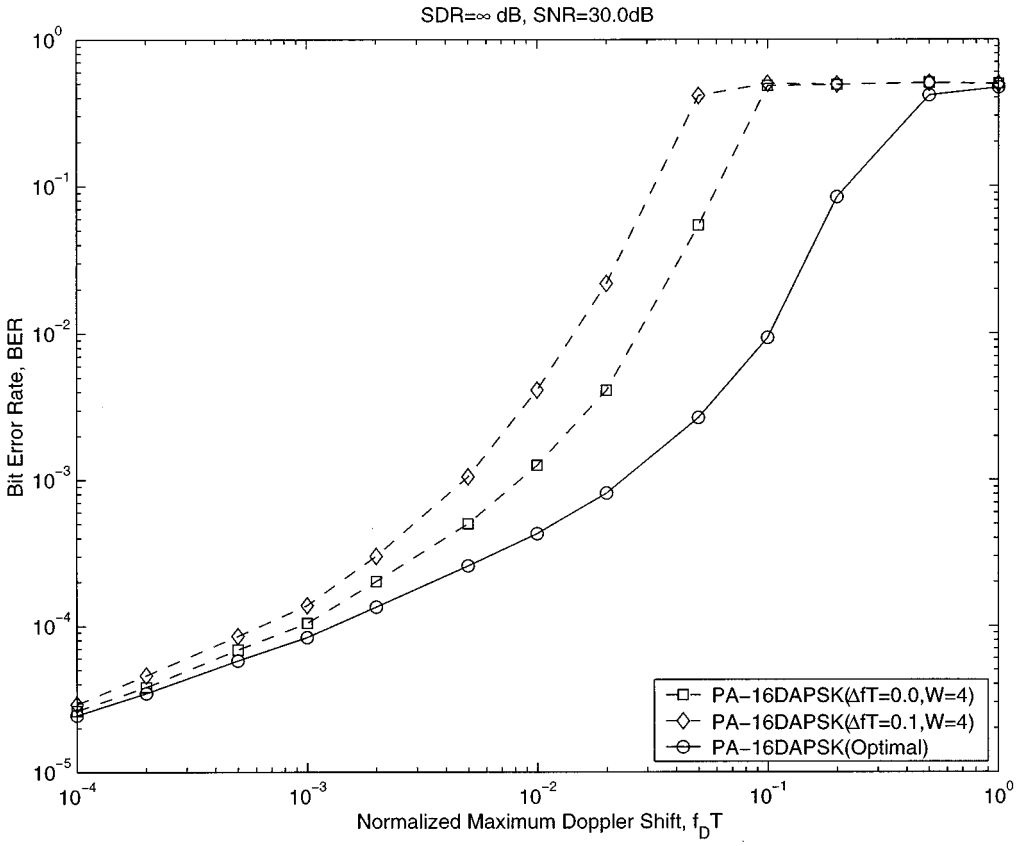

Fig. 11. BER performance versus normalized maximum Doppler shift f_DT in frequency-nonselective fading environments (SDR $= \infty$ dB and SNR $= 30$ dB).

$\pm 1/2N_p$, where N_p is equal to the possible phase number of signals. The boundaries for DD-16DPSK and DD-16DAPSK signals are 1/32 and 1/16, respectively. A theoretical boundary of the normalized frequency offset for the proposed scheme is $(1-\alpha)/2$, where α is the rolloff factor of the matched filter. In the simulations, $\alpha = 0.5$, so the boundary for PA-16DAPSK signals is 0.25.

Fig. 11 shows that the BER performance versus the fading rate f_DT in frequency-nonselective fading environments (SDR $= \infty$ dB and SNR $= 30$ dB). Since the "Optimal" scheme is optimal only for the channel estimation process, the noise term still exists. The signal energy varies rapidly with the increase of fading rate. Thus, the BER performance of the PA-16DAPSK signal in the "Optimal" scheme is dominated by the noise. Furthermore, the error of channel estimation increases with the fading rate. Therefore, the BER performances of PA-16DAPSK signals with $W = 4$ are degraded severely by the estimation error and the noise with the increase of the fading rate.

B. Frequency-Selective Fading Channels

Several simulations have been finished to show the BER performance in the frequency-selective fading environments (SDR $< \infty$ dB and $T_D/T > 0.0$). Fig. 12 shows the BER performance versus the main-path-to-delayed-path power ratio SDR in frequency-selective fading environments (SNR $= 30$ dB and $f_DT = 0.001$) with the normalized delay T_D/T of 0.125. Fig. 13 shows that the BER performances versus the normalized delay T_D/T between the main path and delayed path in frequency-selective fading environments with the equal-power assumption (SNR $= 30$ dB, SDR $= 0$ dB, and $f_DT = 0.001$). From the simulation results, we observe that the BER performance is degraded with the increase of the normalized delay T_D/T and the decrease of the main-path-to-delayed-path power ratio SDR. However, the performance of the PA-16DAPSK signal is the best among the signals under test.

V. Conclusion

In this paper, a novel channel estimation and compensation technique, combining the fading estimation and frequency offset estimation, is investigated for a preamble-assisted DAPSK transmission system in mobile environments. The received preamble symbols are used to estimate the combined distortions caused by multipath fading and frequency offset. The detected data symbols as well as the preamble symbols are used to enhance the accuracy of estimation process. A moving average filter with a suitable window size is employed in the channel estimation process.

Several simulations have been completed to show the improvement in the suppression of frequency offset. Computer simulation results show that the tolerance of frequency offset for 16-DAPSK signals can be increased from 0.0625 to 0.25 by the proposed channel compensation technique. From the computer-simulation results in the frequency-nonselective fading environments (SDR $= \infty$ dB), we observe that the error of the channel estimation is increased and the BER performance is degraded with the increase of the fading rate f_DT. In the frequency-se-

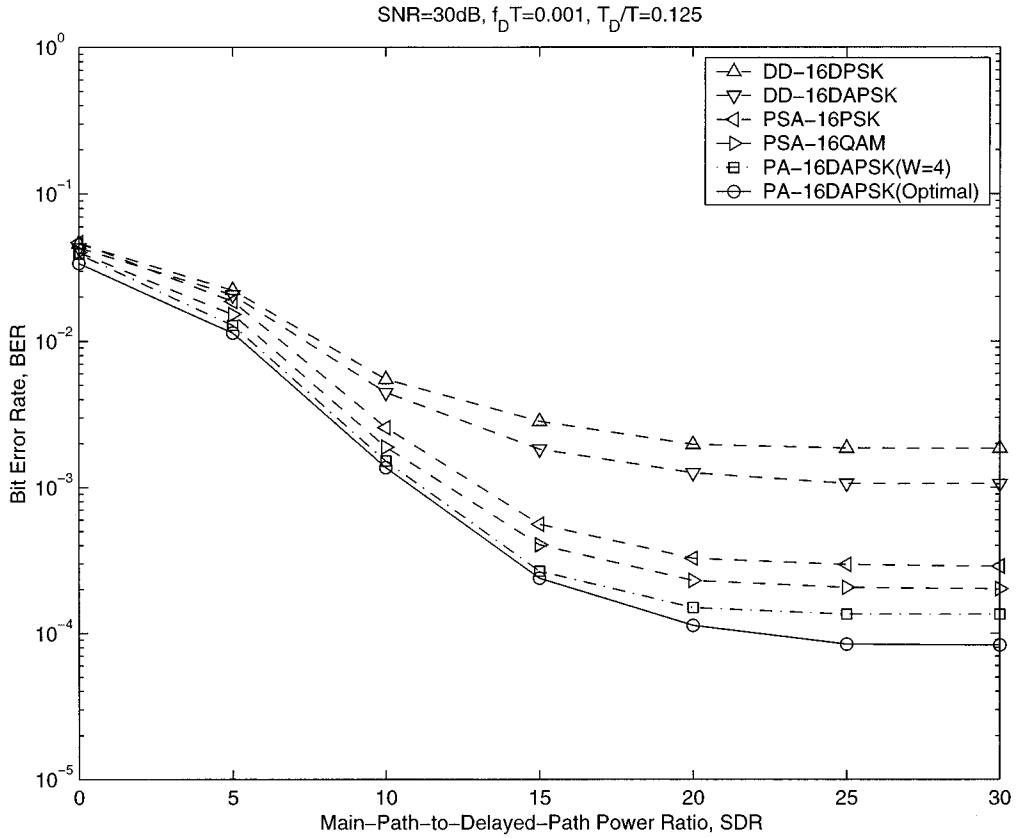

Fig. 12. BER performance versus main-path-to-delay-path power ratio SDR in frequency-selective fading environments (SNR $= 30$ dB and $f_D T = 0.001$) with normalized delay $T_D/T = 0.125$.

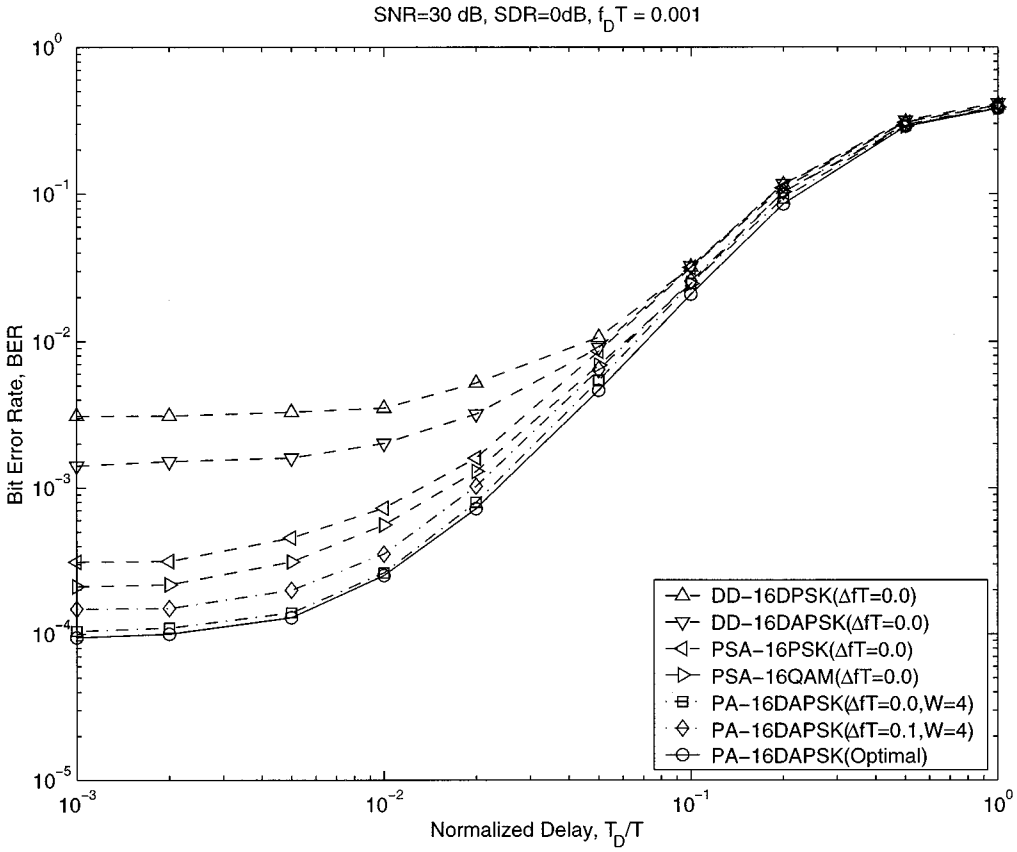

Fig. 13. BER performance versus normalized delay T_D/T in frequency-selective fading environments (SDR $= 0$ dB, SNR $= 30$ dB, and $f_D T = 0.001$).

lective fading environments (SDR $< \infty$ dB and $T_D/T > 0.0$), the BER performance is degraded with the increase of the normalized delay T_D/T and the decrease of the main-path-to-delayed-path power ratio SDR. However, the performance of the PA-16DAPSK signal is the best among the signals under test.

ACKNOWLEDGMENT

The authors are grateful to the editor and the anonymous reviewers for their helpful comments and suggestions.

REFERENCES

[1] W. T. Webb, L. Hanzo, and R. Steele, "Bandwidth efficient QAM schemes for Rayleigh fading channels," *Proc. Inst. Elect. Eng.*, pt. I, vol. 138, no. 3, pp. 169–175, June 1991.
[2] W. T. Webb, "Modulation method for PCNs," *IEEE Commun. Mag.*, vol. 30, pp. 90–95, Dec. 1992.
[3] H. Aghvami, "Digital modulation techniques for mobile and personal communication systems," *Electron. Commun. Eng. J.*, pp. 125–132, June 1993.
[4] W. T. Webb and L. Hanzo, *Modern Quadrature Amplitude Modulation*. New York: IEEE Press, 1994.
[5] W. C. Jakes, Ed., *Microwave Mobile Communications*. New York: IEEE Press, 1974.
[6] J. P. McGeehan and A. J. Bateman, "Phase locked transparent tone-in-band (TTIB): A new spectrum configuration particularly suited to the transmission of data over SSB mobile radio networks," *IEEE Trans. Commun.*, vol. 32, pp. 81–87, Jan. 1984.
[7] P. M. Martin *et al.*, "The implementation of a 16QAM mobile data system using TTIB-based fading correction techniques," in *Proc. IEEE Vehicular Technology Conf.*, Philadelphia, PA, 1988, pp. 71–76.
[8] J. K. Cavers, "An analysis of pilot symbol assisted modulation for Rayleigh fading channels," *IEEE Trans. Veh. Technol.*, vol. 40, pp. 686–693, Nov. 1991.
[9] S. Sampei and T. Sunaga, "Rayleigh fading compensation for QAM in land mobile radio communications," *IEEE Trans. Veh. Technol.*, vol. 42, pp. 137–147, May 1993.
[10] H. K. Lau and S. W. Cheung, "Pilot-symbol-aided 16PSK and 16QAM for digital land mobile radio systems," *Wireless Personal Communication*, vol. 8, pp. 37–51, 1998.
[11] W.-T. Kuo and M. P. Fitz, "Designs for pilot-symbol-assisted burst-mode communications with fading and frequency uncertainty," *Int. J. Wireless Inform. Networks*, vol. 1, pp. 239–252, Oct. 1994.
[12] ——, "Frequency offset compensation of pilot symbol assisted modulation in frequency flat fading," *IEEE Trans. Commun.*, vol. 45, pp. 1412–1416, Nov. 1997.
[13] W. J. Weber, "Differential encoding for multiple amplitude and phase shift keying systems," *IEEE Trans. Commun.*, vol. COM-26, pp. 385–391, Mar. 1978.
[14] A. R. Nix, R. J. Castle, and J. P. Mcgeehan, "The application of 16APSK to mobile fading channels," in *Proc. IEE 6th ICMRPC*, 1991, pp. 233–240.
[15] F. Adachi and M. Sawahashi, "Performance analysis of various 16 level modulation schemes under Rayleigh fading," *Electron. Lett.*, vol. 28, no. 17, pp. 1579–1581, August 1992.
[16] Y. C. Chow, A. R. Nix, and J. P. Mcgeehan, "Analysis of 16-APSK modulation in AWGN and Rayleigh fading channel," *Electron. Lett.*, vol. 28, no. 17, pp. 1608–1610, August 1992.
[17] R. J. Castle and J. P. McGeehan, "A multilevel differential modem for narrowband fading channels," in *Proc. 39th IEEE Vehicular Technology Conf.*, May 1992, pp. 104–109.
[18] F. Adachi, "Error rate analysis of differentially encoded and detected 16APSK under Rician fading," *IEEE Trans. Veh. Technol.*, vol. 45, pp. 1–11, Feb. 1996.
[19] C.-D. Chung, "Differential amplitude and phase-encoded QAM for the correlated Rayleigh-fading channel with diversity reception," *IEEE Trans. Commun.*, vol. 45, pp. 309–321, Mar. 1997.
[20] F. Adachi and M. Sawahashi, "Decision feedback differential detection of 16 DAPSK signals," *Electron. Lett.*, vol. 29, pp. 1455–1457, Aug. 1993.
[21] T. Suzuki and T. Mizuno, "Multiple-symbol differential detection for differentially encoded amplitude modulation signals and its application to 16 DAPSK," *Electron. Commun. Jpn.*, pt. 1, vol. 78, no. 8, pp. 66–75, 1995.
[22] K. Nemoto and I. Sasase, "Differential detection for 16 amplitude/phase shift keying (16 DAPSK) using Viterbi algorithm," *Electron. Commun. Jpn.*, pt. 1, vol. 79, no. 1, pp. 74–81, 1996.
[23] C.-D. Chung, "Noncoherent detection of preamble-signal-assisted differentially phase-encoded APSK signals," *IEEE Trans. Commun.*, vol. 46, pp. 1266–1270, Oct. 1998.
[24] "Electronic industries association specification IS-54, dual-mode subscriber equipment compatibility specification", EIA Project 2215, Dec. 1989.

Der-Zheng Liu (S'96) received the B.S. degree in electrical engineering from National Cheng Kung University, Tainan, Taiwan, R.O.C., in 1993 and the M.S. degree in electronics engineering from National Chiao Tung University, Hsinchu, Taiwan, in 1995, respectively, where he is currently pursuing the Ph.D. degree.

His research interests include digital signal processing, wireless communications, and related circuits design.

Che-Ho Wei (S'73–M'76–SM'87–F'96) received the B.S. and M.S. degrees in electronic engineering from National Chiao Tung University (NCTU), Hsinchu, Taiwan, R.O.C., in 1968 and 1970, respectively, and the Ph.D. degree in electrical engineering from the University of Washington, Seattle, in 1976.

From 1976 to 1979, he was an Associate Professor at NCTU, where he is now a Professor and Vice President of the university. During 1979 to 1982, he was the Engineering Manager of Wang Industrial Company in Taipei. He was the Chairman of the Department of Electronics Engineering of NCTU from 1982 to 1986 and Director of Institute of Electronics from 1984 to 1989. He was on leave at the Ministry of Education and served as the Director of the Advisory Office from September 1990 to July 1992. He was Dean of Research of NCTU from August 1993 to July 1995 and Dean of the College of Electrical Engineering and Computer Science from August 1995 to July 1998. His research interests include digital communications and signal processing, and related circuit design.

Dr. Wei was the Founding Chairman of the Taipei Chapter of the IEEE Circuits and Systems Society and IEEE Communication Society. He was a member of the Board of Governors, IEEE Circuits and Systems Society, from 1992 to 1994. He received the Distinguished Research Award from the National Science Council, R.O.C., in 1990 to 1996. He received the Distinguished Engineering Professor Award from the Chinese Institute of Engineers in 1995. He received the Academic Achievement Award from the Ministry of Education, R.O.C., in 2000. He received the IEEE Third Millennium Medal and IEEE Circuits and Systems Society Golden Jubilee Medal, 2000.